IET Electrical Systems in Transportation

Review Article

Thermal management of electric machines

ISSN 2042-9738
Received on 4th December 2015
Revised 16th May 2016
Accepted on 27th June 2016
doi: 10.1049/iet-est.2015.0050
www.ietdl.org

Yinye Yang[1] ✉, Berker Bilgin[1], Michael Kasprzak[1], Shamsuddeen Nalakath[1], Hossam Sadek[1], Matthias Preindl[1], James Cotton[1], Nigel Schofield[1], Ali Emadi[1]

[1]McMaster Institute for Automotive Research and Technology (MacAUTO), Faculty of Engineering, McMaster University, Hamilton, ON L8P 0A6, Canada

✉ *E-mail: yangy9@mcmaster.ca*

Abstract: Electric machines have broadly been used in many industries including the transportation industry. With the evolving trend of electrification in transportation, electric machines with higher power density and higher efficiency are demanded and, thus, more stringent thermal management requirements are needed for electrified vehicle applications. This study comprehensively presents various important aspects of thermal management in electric machines with the main focus on transportation applications. Design considerations, challenges, and methods for enhanced thermal management are discussed. Fundamental thermal properties of common materials are presented and sources of losses in various parts of machines are explained. Furthermore, typical cooling techniques and thermal analysis approaches for electric machines are reviewed in detail. This study will serve as a reference guideline for machine designers, who are interested in thermal management, and for thermal researchers working on electric machines.

1 Introduction

Electric machines are used in many industries including home appliance, medical and health, food, energy, mining, machining, manufacturing, and transportation including automotive and aerospace applications. They generate almost all electric energy (with the exception of fuel cells, photovoltaic panels, and batteries) and provide about 60% of total energy conversion from electric form to mechanical form [1]. Throughout the technology development for more than a century, electric machines have evolved into various configurations under both DC and AC machine categories. Brushed DC machines were among the most popular machines until the 1970s and the advent of brushless DC machines with power electronic devices took place. The removal of mechanical brushes and commutators enables higher efficiency and reliability, contributing to the extensive applications of brushless DC machines in a wide range of fields [2]. On the other hand, AC induction machines (IMs) have widely been used in industrial drives such as fans, pumps, and compressors, while synchronous AC machines are extensively used in generating electricity in power plants and automotive alternators [2]. In addition, various other machine configurations exist including switched reluctance machines (SRMs), synchronous reluctance machines, transverse flux machines, axial flux machines and so on [3].

Thermal management of electric machines is critical in order to improve machine performance and ensure reliability. Historically, machine thermal management relies on design experience and simple sizing methods such as winding current density and operating conditions to a large extent [4]. These methods typically apply large safety factors to avoid the worst heating scenarios and result in over-design of the cooling system or over-sizing of the machine. With the evolving trend of electrification in transportation, there is growing demand for electric machines in automobiles [5], locomotives [6], agriculture machines [7, 8], and aerospace [9] ranging from starter-generators to traction propellers [10]. Machines with higher efficiency, wider speed range, and better power density are in demand while smaller size, lighter weight, and lower cost are desired [11, 12]. All these targets require optimised machine designs and, thus, better thermal management is of exceptional importance. In addition, machines with variable load and speed instead of steady-state operations are broadly applied. Transient heat profiles lead to more stringent thermal management requirements and integrated cooling techniques [13, 14].

Thermal management has been applied as a general practice in the manufacturing of electric machines. However, it has not been comprehensively documented in academic research papers. The majority of the papers focus on one particular aspect of thermal analysis applying to one specific machine topology. Liao *et al.* [15] discussed thermal analysis for design of high performance motors. Howey *et al.* [16] analysed air-gap convection in rotating electrical machines in an effort to predict machine temperature distribution. Bennion and Cousineau [17] conducted a sensitivity study on traction motor cooling. It is difficult to find a paper inclusively covering all the aspects of thermal management in electric machines. Only until recently, Boglietti *et al.* [18] published a survey describing the evolution and modern approaches to thermal analysis of electric machines. It reviewed various thermal analysis approaches in great detail. However, it focused on the analytical level without giving too much information about practical design and manufacturing considerations. In addition, Moreno *et al.* [19] presented thermal management and reliability of automotive electric traction-drive systems. However, they focused on limited parts of thermal management in electric machines. Thus, this paper aims to comprehensively discuss different aspects of electric machine thermal management and general techniques applied. Fundamental loss generation principles, material properties, analysis techniques, cooling methods, and design considerations will be covered extensively. The rest of the paper is structured as follows: Section 2 discusses the compound design considerations for electric machine thermal management, challenges, and approaches to enhance the thermal performance. Section 3 discusses typical material thermal properties and Section 4 explains fundamental loss generation mechanism in different parts of electric machines. Typical cooling techniques are reviewed in Section 5 and various thermal analysis approaches are then presented in Section 6. Finally, Section 7 concludes the paper with findings and contributions. The authors hope this paper will serve as a reference guideline for machine designers who are interested in thermal management and for thermal researchers who are interested in machine technologies.

© The Institution of Engineering and Technology 2016

Fig. 1 *Thermal management in electric machines*

2 Thermal management considerations

Thermal management is a complex, but crucial aspect in electric machine design. For example, high temperature results in high copper resistance and hence high losses in the windings. Excessive temperature reduces the remanence and coercivity of permanent magnets (PMs), affecting machine torque and demagnetising the magnets [20]. Inefficient cooling system leads to faster insulation degradation and increased winding failure rates due to increased thermal cycles [2]. It is a rule of thumb that 10°C temperature rise halves the life expectancy of the electric machine [21]. In addition, lamination stacks, coils, and end turns all have a direction-dependent thermal conductivity [22]. Non-thermally conductive materials such as magnet adhesives and winding insulations may also result in local heat concentration. Therefore, effective thermal management improves electric machine performance and ensures reliable machine operation, while poor thermal management results in performance degradation, accelerated machine wear, and even may cause machine breakdown.

Thermal management requirements in electric machines vary depending on the application. For small mechatronic drives in automotive, medical applications, and home appliances, motors typically work under light load within a short period of time. Thus thermal management is primarily targeted to enable efficient heat removal at transient conditions. For fixed speed industrial drives where there is typically no space or environment temperature limit, natural convection and forced convection are often applied. This is a relatively inexpensive and sufficient solution for steady-state applications. For power dense wind turbine generators, where space is limited and maintenance access is difficult, thermal management is critical to ensure the continuous operation and meet the service life. Liquid cooling channels in both the generator and the gearbox are typically implemented, and a heat exchanger is utilised to dissipate heat to the ambient. For traction motor applications, separate cooling systems may be required such that a lower-temperature cooling loop is used for electric machine and power electronics, while a higher-temperature loop is used for the engine [19]. In electrified powertrain applications, electric traction motors are usually integrated into the transmission. Thus, transmission oil can be utilised for both the transmission cooling and electric machine cooling.

Different thermal management requirements are necessary for different types of electric machines. In general, rotor is more difficult to cool during operation due to lack of accessibility. SRM has the simplest machine configuration where there is no magnet or windings on its rotor, and therefore SRM has the highest capacity in terms of high temperature resistance [23]. In comparison, IM generates significant a amount of heat in the rotor as current is induced in square-cage bars or wounded rotor windings. Without proper thermal management, excessive heat can build up and transfer to the neighbouring components, leading to negative impacts on the bearing life. Similarly, special thermal concerns should be given to the PM machines as local heat concentration may occur around the magnets. High temperature can affect the magnet performance and result in potential demagnetisation [14]. For brushed DC machines, maximum load and speed should be controlled to prevent excessive heat generated on the brushes and commutators.

To enhance thermal management in electric machines, it is essential to resolve challenges from all aspects including the heat sources, the heat dissipation paths, and the heat removal sinks, as shown in Fig. 1. Heat generated from iron losses can be reduced by thinner-cut laminations, advanced steel materials such as cobalt–iron (CoFe) alloys, and well-controlled annealing method [24, 25]. Decreasing the amount of alloy materials can increase the thermal conductivity and magnetic performance of laminations, though at the expense of increased resistivity and eddy currents losses in the laminations [26]. In addition, magnet losses can be reduced by segmenting magnets in the axial direction. Lower copper losses can be achieved by lower winding temperature. On the other hand, thermal management can be enhanced by facilitating the heat dissipation along the thermal path. Advanced thermal conductive materials can be incorporated to reduce contact resistance. Thermal fillings can be used to increase the heat transfer coefficient. Larger heat dissipation surface areas can be considered for better heat dissipation. Cooling paths can be integrated to target at local areas of heat concentration and so on [27]. Finally, thermal sink is also critical for electric machine thermal management. Both active cooling and passive cooling can be applied to remove the heat from the machine. Increasing coolant flow rate and jet cooling velocity typically increases the heat transfer coefficients [19]. The configurations of water jackets and housing fins also determine the cooling efficiency. More details will be presented in Section 5.

In summary, good thermal management of electric machines requires careful design considerations from various perspectives. The following sections will describe the issues in detail based on fundamental material properties, heat generations, cooling methods, and typical thermal analysis used for electric machine thermal management.

3 Material thermal properties

The temperature rise in an electric machine is usually limited by the thermal properties of the materials. Maximum temperature specification of the machine, manufacturing techniques and also the machine topology play an important role in material selection. Material thermal properties should be carefully evaluated in a thermal management system design process.

3.1 Conductors

The largest amount of losses in an electric machine is usually due to the losses in the conductors. This includes the copper losses in the stator conductors and, especially in IMs, followed by the losses in the rotor conductors [28]. Magnet wires are widely used in electric machines to create the stator magnetic field. The insulation around the copper conductor enables the contact between the wires without causing any electrical short circuit. Magnet wire insulation, in general, is made of organic material, which softens at a lower temperature than copper or electrical steel. The mechanical strength of the insulation is also much lower than copper or steel [29]. Therefore, electrical insulation around the conductors generally creates the limit on the lifetime of the stator winding.

American National Standards Association standardises magnet wires [30]. The selection of the correct magnet wire is highly dependent on the machine operating condition, such as the thermal class, insulating (or coating) material, current density, frequency, voltage and so on. The lifetime of the insulation reduces by half for every 10 °C increase in the temperature over its thermal class. The insulating layers, the so-called enamels or films, are bonded on the copper or aluminium conductor. They are made up of different types of resins and define the thermal class of the magnet wire [31]. Table 1 lists the thermal classes of round magnet wires and the insulation materials based on some of the widely used ANSI/NEMA MW1000-2015 standards [30]. Round magnet wires form a random-wound machine winding, which is generally applied below 690 V phase-to-phase voltage. Beyond this point, rectangular wires

© The Institution of Engineering and Technology 2016

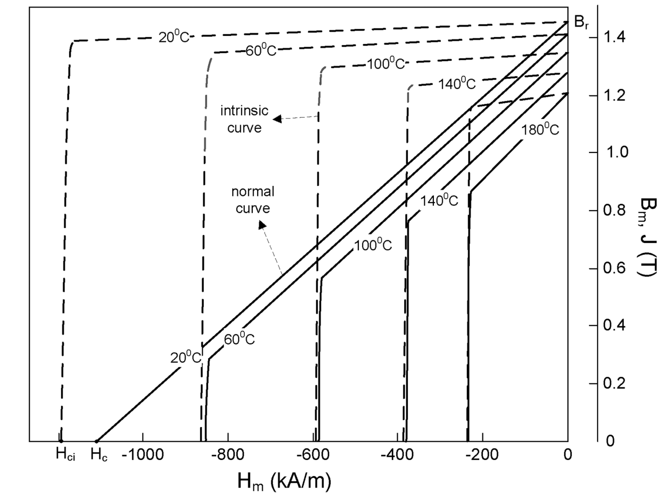

Fig. 2 *Demagnetisation and characteristic curves of a PM (TDI Neorec53B iron-based rare-earth magnet) [36]*

are used and they are formed, so that the turn-to-turn voltage does not exceed the dielectric breakdown of the insulation system [29]. It should be noted that polyester (amide) (imide) in Table 1 means that the insulating thermoplastic has all three functional groups of ester, amide, and imide in one polymer.

For most of the magnet wire thermal classes, different insulation materials are available. The choice of the correct insulation material is dependent on many factors, such as oil resistance, flexibility, resistance to common solvents, solderability, thermal stability, heat shock capability, windability, resistance to moisture, salt water resistance and so on. For example, polyurethane is not used for high temperature and high current applications. Polyester (amide) (imide) underlying coating with polyamideimide superimposed coating (e.g. MW35-C) provides high resistance to chemicals and moisture [32]. Glass fibres can provide flexibility and they are available in larger diameters [33]. These characteristics help in defining the proper magnet wire for the given requirements, such as oil-cooling, high winding stresses,

Table 1 Thermal classes and insulating materials of round copper magnet wires according to ANSI/NEMA MW1000-2015 [30]

Magnet wire thermal class	Standard	Insulating material	
		Underlying coating	Superimposed coating
105	MW15-C	polyvinyl acetal-phenolic	
130	MW28-C	polyurethane	polyamide
155	MW79-C	polyurethane	
	MW80-C	polyurethane	polyamide
	MW41-C	glass fibre covered	
180	MW76-C	polyester (amide) (imide)	polyamide
	MW77-C	polyester (imide)	
	MW78-C	polyester (imide)	polyamide
	MW82-C	polyurethane	
	MW83-C	polyurethane	polyamide
	MW50-C	glass fibre covered	
200	MW74-C	polyamide (amide) (imide)	
	MW35-C	polyester (amide) (imide)	polyamideimide
	MW44-C	glass fibre covered	
220	MW61-C	aromatic polyamide	
	MW37-C	polyester (amide) (imide)	polyamideimide
	MW81-C	polyamideimide	
240	MW16-C	aromatic polyimide	

high overload capabilities, high temperature operation, automated winding process and so on [32].

Magnet wires have standardised dimensions, which are categorised with American Wire Gauge (AWG). Different standards offer different AWG values, but for the same AWG number, the wire size should be the same even though the insulating material is different. Magnet wires have an insulation layer (or build), which defines the grade of the wire. Generally four different grades are available: single-, heavy-, triple-, and quadruple-build, in the order of increasing insulation thickness. For different grades, the magnet wire size is still standardised. The dielectric breakdown voltage of the magnet wire is dependent on the insulation grade: the higher the grade, the higher the breakdown voltage. However, the insulation material itself also has an impact on the breakdown voltage [34].

It should be noted that cost is an important factor in selecting the proper magnet wire. Magnet wires have the same dimensions for the same AWG value for different thermal classes, but the cost generally increases as the thermal class increases.

In addition to the conductors on the stator, squirrel-cage IMs have rotor conductors, which are conventionally manufactured by die-casting aluminium in the rotor slots. At room temperature, copper has 70% higher conductivity than that of aluminium. Therefore, aluminium die-casted IMs would naturally end up with higher rotor copper losses. For the same power density, this might require a more aggressive thermal management system. However, besides the electrical conductivity, copper has higher coefficient of thermal expansion (CTE) when compared to aluminium. The difference between the CTE of copper and steel would apply fatigue stress at the copper–steel interface [35]. Thermal management system should be properly designed in a copper-cage IM to avoid cracks on the conducting bars throughout the thermal cycling of the machine. It should be also noted that die-casting of copper is a challenging process due to the higher melting temperature and density of copper [35].

3.2 Permanent magnet

The magnetic properties of PMs are highly dependent on the operating temperature. In electric machines, maximum operating temperature should be defined to maintain stable operation of the magnet.

Iron based rare-earth magnets (NdFeB) are widely used in traction machines due to their high-energy product and high coercivity. However, the performance of NdFeB magnet is very sensitive to temperature. Normal and intrinsic curves in Fig. 2 show that the flux density and coercivity of NdFeB magnet reduces as the temperature increases. This means that, the output torque and the capability of tolerating the negative field from the stator windings are highly dependent on the magnet temperature [3].

From Fig. 2, it can be observed that at high temperatures, the intrinsic coercivity, H_{ci} of the magnet decreases. Depending on the external field and the permeance coefficient, if the load line crosses the magnetisation curve below the knee point, magnet loses some of its magnetisation [37]. This is an irreversible loss and it is caused by the reversal of domains, which were initially aligned in the direction of magnetisation. Irreversible losses are dependent on the operating conditions, temperature and how long magnet is exposed to that temperature. Irreversible losses can be only recovered by re-magnetising the magnet. In PM machines, the temperature, loading conditions and irreversible-loss data provided by the magnet manufacturer should be carefully evaluated to design proper thermal management system [38].

Cobalt-based rare-earth magnets (SmCo) are also used in electric machine applications. SmCo has higher Curie temperature as compared to NdFeB; therefore it can operate at temperatures up to 250 °C. However, SmCo has lower coercivity and energy product when compared to NdFeB, and is more expensive. Aluminium–nickel–cobalt (AlNiCo) magnets can also operate at high temperatures, but they have lower energy product when compared to NdFeB and SmCo. Unlike other magnets, ferrite magnets have positive temperature coefficient (PTC) for the coercivity [38]. The coercivity of ferrite magnets increases as the

© The Institution of Engineering and Technology 2016

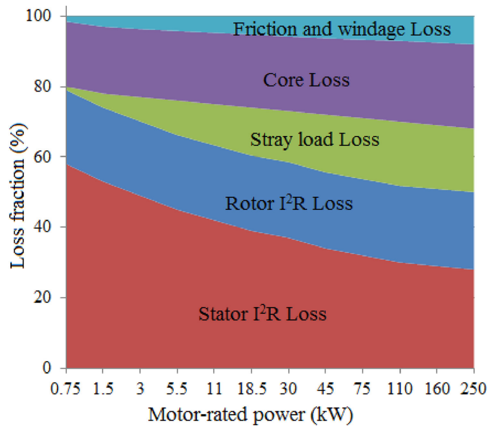

Fig. 3 *Loss fraction in typical four-pole IMs at 50Hz*

temperature increases. Therefore, both low and high temperature performances should be evaluated carefully when designing a thermal management system for electric machines with ferrite magnets.

It should be also noted that CTE of PMs is twice as high as that of silicon steel. Without proper temperature control, the shear stress on the magnets can cause deterioration on the machine performance and potentially cracks on the magnet [39].

3.3 Silicon steel

In a thermal management system design, the thermal class of the coils and the maximum allowable temperature of the PMs generally define the maximum operating temperature of the machine. The magnetic properties of electrical steels usually change drastically near the Curie temperature (770 °C for iron). At any magnetic field intensity, the magnetic flux density of the steel reduces as the temperature approaches to Curie point. In [40], it was shown that, in case of non-oriented steel, the permeability of electrical steel did not change much under about 500 °C. This temperature is much higher than the maximum temperature PMs and magnet wires usually handled.

It is also important to note that the surface insulation of electrical steels should handle the annealing temperatures during the manufacturing process. Electrical steels have surface insulation to increase the resistivity between laminations and, hence, reduce the eddy currents. Annealing is a heat treatment process to eliminate the stress due to the plastic deformation on the laminations and helps to return the magnetic properties of the steel back to the stress-free conditions [41]. American Society for Testing and Materials (ASTM) standardises the classification of insulating coatings for electrical steels [42]. The insulation material, annealing temperature, duration, and pressure during the annealing process should be carefully defined not to deteriorate the surface insulation of the electrical steel. Otherwise, the resistivity of the insulation might be affected leading to higher eddy current losses.

Table 2 Properties of liquid coolants for electric machine applications [39]

Coolant type	Specific heat, K/kg K	Density, kg/m^3 at 1 atm	Therm. cond., W/m K	Dynamic viscosity (Pa s) × 10^{-3} at 20 °C
water	4181	997	0.613	1.002
methanol/water (40/60 by weight)	3560	935	0.4	2.0
ethanol/water (44/56 by weight)	3500	927	0.38	3.0
ethylene glycol/ water (50/50 by volume)	3350	1069	0.39	3.4
engine oil	1765	887	0.138	81.3

3.4 Insulation materials

In electric machines, slot liner and slot wedges are used to prevent possible winding-to-ground short circuit faults. These insulation materials are usually made of aramid or Mylar layered paper. Nomex is an insulation paper supplied by DuPont for slot insulation. It has higher mechanical strength, better flexibility, higher chemical and moisture resistance, and high dielectric breakdown strength at high temperatures [43]. Nomex paper is also utilised in magnet wire film insulation, for thermal class 220. The thickness of the slot insulation material ranges between 0.1 and 0.65 mm.

Encapsulation of the stator via vacuum pressure impregnation process helps to improve the transmission of heat from the copper to the stator core by replacing the air pockets with varnish or thermally conductive epoxy [39]. It also provides higher dielectric and mechanical strength, chemical and heat resistance [29].

3.5 Coolant

The heat transfer coefficient of the thermal management system depends on many parameters, including the geometry, flow rate, and also the type of the coolant. For the same operating conditions, such as flow rate and temperature, air cooling has a much lower heat transfer rate when compared to liquid cooling. However, it is the preferred choice in small to medium power applications. Very high heat transfer coefficients can still be obtained with advanced air cooling techniques, such as air jet impingement cooling [39].

Thermophysical properties of air change with temperature and pressure. The thermal conductivity and specific heat of air increase with temperature. In addition, the density of air decreases with increasing temperature. Air density is an important parameter in defining the mass flow rate and pressure loss of the cooling system [44].

Liquid cooling has been acknowledged as a more effective method to achieve higher heat transfer coefficients. When selecting the coolant for the liquid cooling system, thermophysical properties, dielectric strength, and chemical compatibility of the coolant play important role. Table 2 shows the properties of some of the liquid coolants used in electric machine applications. With the highest specific heat, water can transfer the highest amount of heat with the same flow rate. It also has low viscosity, which maintains lower fluid flow resistance [39]. However, water cannot be used for direct cooling, since it is electrically conductive and may cause corrosion over time.

4 Loss generation in electric machines

The losses in electric machines are generated by different physical mechanisms. They are typically classified as copper, iron core, magnet, mechanical, and stray losses. The copper loss results from Joule heating due to the resistivity of the conductors. The iron losses are caused by the time-varying magnetic field that yields hysteresis and eddy current losses. To fully capture the electromagnetic losses, additional loss mechanisms need to be taken into account, viz. the skin effect, proximity effect, magnet eddy current, excess core loss, and stray loss. Electric machines feature also mechanical losses, in particular friction and windage losses. Fig. 3 shows the typical losses of different rated-power four-pole IMs at 50 Hz [45]. The loss mechanisms of electrical machines are discussed in the next subsections and computational methods to estimate losses are introduced.

4.1 Copper loss

Copper loss is a major loss component in all electric machines, especially at high torque operation. Most machines feature copper losses in both the stator and rotor, except for PM and reluctance machines. In addition, frequency dependent skin and proximity effects add to the overall copper losses. The skin effect is caused by eddy currents induced by a conductor's own flux linkage. The

© The Institution of Engineering and Technology 2016

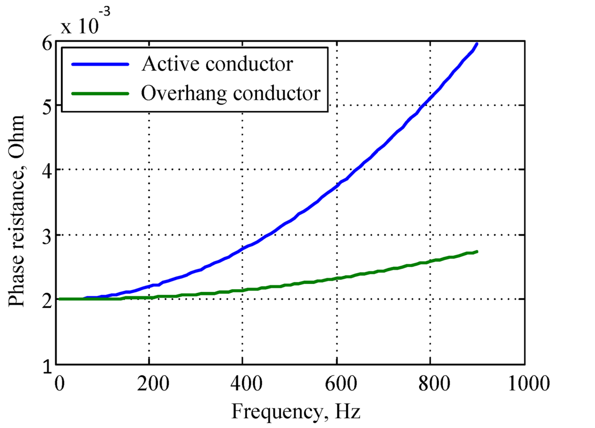

Fig. 4 *Frequency impact on the phase resistance in an example PM machine*

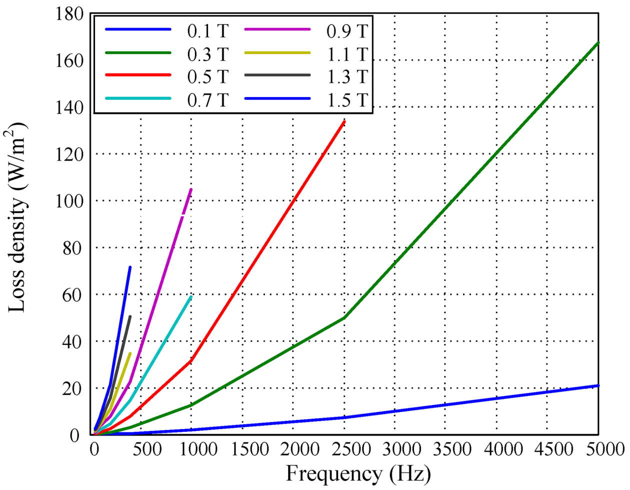

Fig. 5 *Manufacture's loss data for 50CS350 China steel*

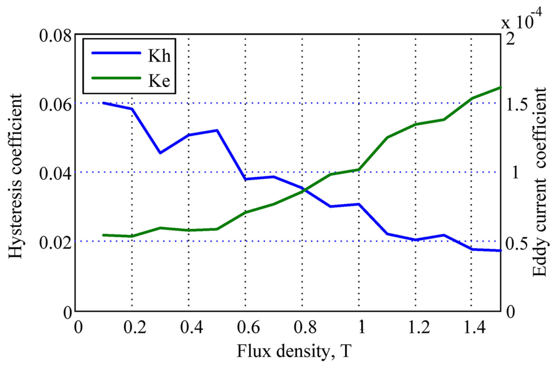

Fig. 6 *Hysteresis and eddy current loss coefficients*

proximity effect is caused by the flux from neighbouring conductors [46]. The skin and proximity effects cause a non-uniform current distribution in conductors, which becomes more extreme as frequency increases. In practice, the copper loss is calculated using the winding resistance parameter. At low frequency, the copper losses are dominated by the Joule effect that is modelled with the DC resistance. Frequency dependent effects are captured introducing equivalent AC resistances [47]:

$$P_{\mathrm{cu}} = m\, I_{\mathrm{p}}^{2}\left(R_{\mathrm{dc}} + R_{\mathrm{skin}}(f) + R_{\mathrm{proximity}}(f)\right) \quad (1)$$

where m is the number of phases, I_{p} is the rms phase current, f is the frequency, R_{dc}, $R_{\mathrm{skin}}(f)$ and $R_{\mathrm{proximity}}(f)$ are the DC, skin, and proximity components of phase resistance, respectively.

The DC component of phase resistance is found through the resistance equation based on the conductor geometry. The AC components are either found analytically [46, 47] or estimated by using finite element (FE) software. The magnetic field strength is low in the overhang region as compared to the active region and, therefore, the proximity effect in the overhang region is typically negligible [46]. The skin effect is approximated as constant throughout overall length of the conductor [46]. The impact of the frequency on the phase resistance of the active and overhang regions is shown in Fig. 4. It should be noted that the phase resistance is also marginally influenced by excitation current especially when the core is saturated [46].

The copper loss increases as the resistance increases with the temperature. The temperature at overhang conductors is higher than the active conductors. The conductors in the slots are surrounded by electrical steel, which has higher thermal conductivity [48]. This provides better heat dissipation in the active region of the coils. Therefore, the heat source by the copper loss is modelled separately for active and overhang regions. The effect of temperature in copper loss model is determined by updating resistivity as a function of temperature [48]

$$\rho_{\mathrm{T}} = \rho_{o}[1 + \alpha\,(T - T_{o})], \quad (2)$$

where ρ_o is the resistivity at initial temperature T_o, α is the temperature coefficient, and T is the final temperature. The updated resistivity is used to compute the resistance components in (1).

4.2 Iron losses

The iron loss is the second major loss component in electric machines. It is typically dominant when a machine operates at higher frequency, i.e. at high speed. Hysteresis and eddy current losses are the main iron loss components. The hysteresis loss is caused by a time-varying magnetic field primarily in major loops. Eddy current loss is caused by the current induced in the core (typically laminations). The difference between classical eddy current and total eddy current losses is defined as excess loss [49]. The harmonic content due to slotting, winding distribution, non-sinusoidal and pulse-width modulation (PWM) excitations cause core losses at higher order frequencies [50, 51].

The Steinmentz equation is primarily used to quantify the core loss. Its coefficients are generally treated as constants. However, variable coefficients are required for predicting core loss for a wide operating region. The coefficients vary with flux density and frequency. Loss data from a core manufacturer for different frequency and flux density is shown in Fig. 5. This data is used to actually find the coefficients. The variation of hysteresis and eddy current coefficients with respect to flux density is shown in Fig. 6. Modified equations are used to account for PWM effects and arbitrary waveforms [52]. The loci of the flux rotation are used to account for rotational loss [53]. The Steinmentz equation that takes harmonic components into account is [54]

$$P_{\mathrm{core}} = \sum_{n} K_{\mathrm{h}n} B_{n}^{1.6}\, nf + K_{\mathrm{e}n} B_{n}^{2}\,(nf)^{2}, \quad (3)$$

where n is the harmonic index, K_{h} and K_{e} are the hysteresis and eddy current loss coefficients, respectively, B is the flux density, and f is the frequency.

The iron loss is distributed throughout the core depending on the amplitude and frequency of local flux density waveform. In AC machines, the main iron losses happen on the stator where the stator teeth and back iron are the major core loss regions. The loss in tooth tips, or pole shoes, is relatively low and it can be neglected while considering thermal design [48]. In comparison, the rotor core loss is typically less since the frequency of the magnetic flux density variation in the rotor core is lower compared to that of the stator. It should be noted that air gap and current harmonics yield alternating rotor flux harmonics causing additional iron losses. For example, in wound field synchronous machines (SMs), the rotor lamination tends to be made from thick steel to reduce manufacturing costs. In this case, the specific rotor core loss can be high in proximity of the air gap [55]. However, these effects can be ignored in some other machines. For example, the large effective

© The Institution of Engineering and Technology 2016

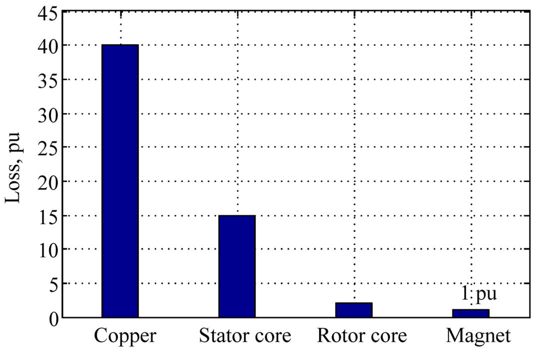

Fig. 7 *Rated losses in an IPM machine*

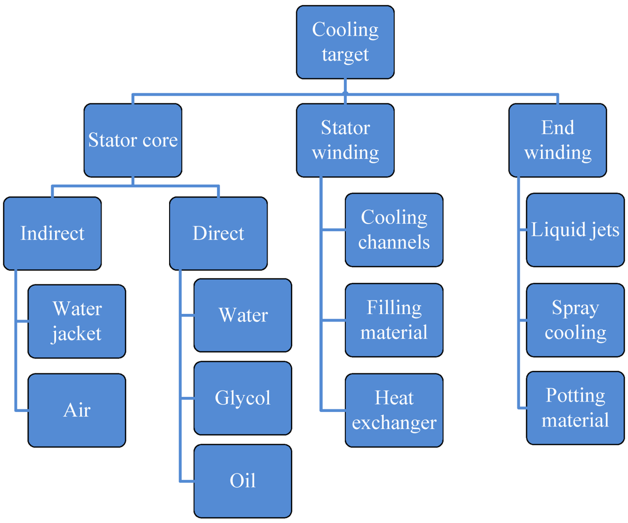

Fig. 8 *Cooling technologies depending on cooling target*

air gap in surface PM machines shields the rotor back iron from flux harmonics [52].

A simple approach to include the core loss in thermal analysis is to consider two heat sources, one is in the stator and other is in the rotor [48]. A detailed approach is to consider many heat sources corresponding to regions classified based on the same core loss density [54]. The values of core losses can be found from analytical equations. Many of the commercial software also provide core loss calculation as part of their post processing.

4.3 Magnet losses

Magnet loss, if applicable, is usually the lowest when compared to other losses in most electric machines. Fig. 7 shows the different losses at the rated condition of an example IPM machine. Despite the low amount, the magnet loss is very critical in thermal aspect. The local magnet temperature can increase significantly as the heat generated by magnets takes a long path to reach the cooling sink causing a large equivalent thermal resistance. Magnet over-temperature can cause irreversible partial or full demagnetisation. In addition, surface mounted magnets are more prone to harmonics than embedded magnets [52]. Typically, magnet segmentation is used to reduce the magnet loss. However, too many layers of segmentation may adversely affect the heat conduction and increase cost.

Eddy currents that are induced in the magnets due to rotor flux variation cause the magnet loss. At no-load, only the air gap reluctance variation causes rotor flux harmonics. At loaded condition, flux harmonics due to non-sinusoidal excitation, distribution, and PWM have to be taken into account. The loss generated by slot harmonics is typically the major contributor to the magnet losses [31]. Assuming that the flux density across the magnet is uniform and neglecting skin effect due to the reaction field, the magnet loss can be calculated according to [56]

$$P_{\text{magnet}} = \frac{V_{\text{m}} W_m^2}{24\,\rho_{\text{m}}} \sum_n B_n^2 \omega^2 n^2, \qquad (4)$$

where V_{m} is the volume of the magnet, W_m is the width, B is the amplitude of flux density for a particular harmonic order, w is the frequency, ρ_{m} is the resistivity of the magnet, and n is the harmonic index. The value of the flux density is either found analytically or by static FE analysis (FEA).

Equation (4) is valid for smaller magnets and low frequency operating machines in which skin effect is negligible. There are many methods reported in the literature that consider the eddy current reaction field in analytical models [56, 57]. The commercial FE software packages also have advanced magnet loss calculation methods. However, magnet segmentation adds complexity to the FEA. Also, the inclusion of fringing-effects gives better magnet loss calculation results, and thus, 3D models are typically preferable [57].

4.4 Mechanical losses

Mechanical loss in electric machines consists of friction and windage losses. Friction losses are mainly caused by the bearings and are thermally relevant. The resulting heat and the heat passing to the ambient via bearing increase the local temperature. This tends to degrade the lubricant and reduce the life of the bearing. The aerodynamic drag experienced by rotor periphery and cooling fan causes windage loss. These losses can be minimised using high quality bearings, lubricants and high-performance fan designs. A general expression for windage and friction losses is [58]

$$P_{\text{fw}} = 2\,D^3 L\, n^3 10^{-6} + K_{fb} G\, n\, 10^{-3} \qquad (5)$$

where D, L and G are outer diameter, length and weight of rotor, respectively, n is the rotational speed, and K_{fb} is the frictional loss coefficient.

5 Cooling techniques for electric machines

Cooling technologies for electric machines can be classified according to the mode of heat transfer: conduction, natural convection, forced convection, radiation, and evaporative cooling; or according to cooling fluid: water, air, oil, and phase change materials; or according to the parts being targeted for cooling: stator core, stator windings, end windings and so on, as shown in Fig. 8. Some of these technologies can be incorporated simultaneously to minimise the temperature of the various critical locations, i.e. hot spots. This section discusses various commonly-used cooling technologies for electric machines.

Dissipating the heat generated within an electric machine to an external heat sink depends on various factors: the mode of heat transfer, the effective heat transfer area and geometry, the working fluid used for cooling, the flow rate and temperature of the cooling media and so on. The simplest cooling technique is dissipating the heat to the ambient by natural convection. Typically, the heat dissipation can be improved by increasing the heat transfer surface area with added fins on the housing. More complicated forced air-cooling system can be used to further increase the heat dissipation. For example, a shaft mounted fan can be employed to enhance the heat transfer from the housing fins, the end windings, and rotor surfaces. However, for high current densities, using air as the cooling fluid may not be sufficient and some form of liquid cooling may be required for better cooling efficiency. Typical rules of thumb for cooling techniques and associated heat transfer coefficients are listed in Table 3 [4, 59]. It is apparent that higher cooling efficiency enables higher current density and hence higher machine output power, however, at the expense of higher system complexity and energy cost.

In terms of the cooling location, stator core cooling is the most commonly used technology in electric machines. It can be divided into direct cooling where the heat is removed directly from the stator core [60, 61], or indirect cooling where the heat is transferred radially and/or axially to the external surfaces and dissipated by the

© The Institution of Engineering and Technology 2016

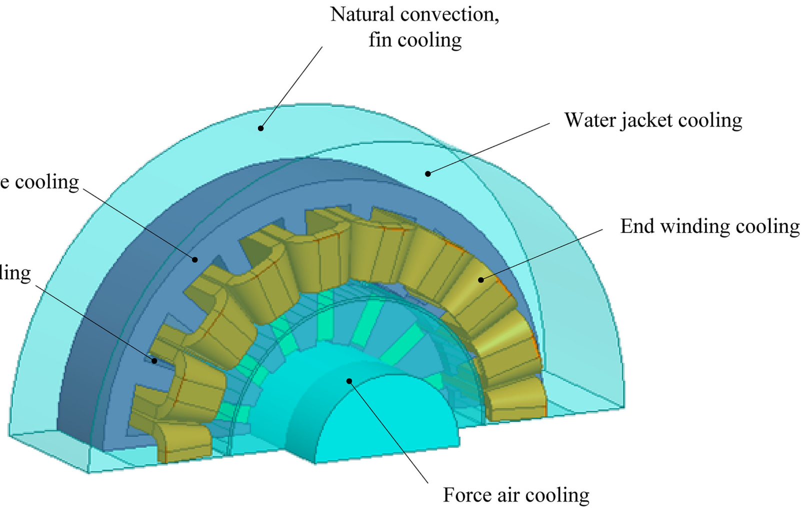

Fig. 9 *Cooling technologies depending on cooling locations*

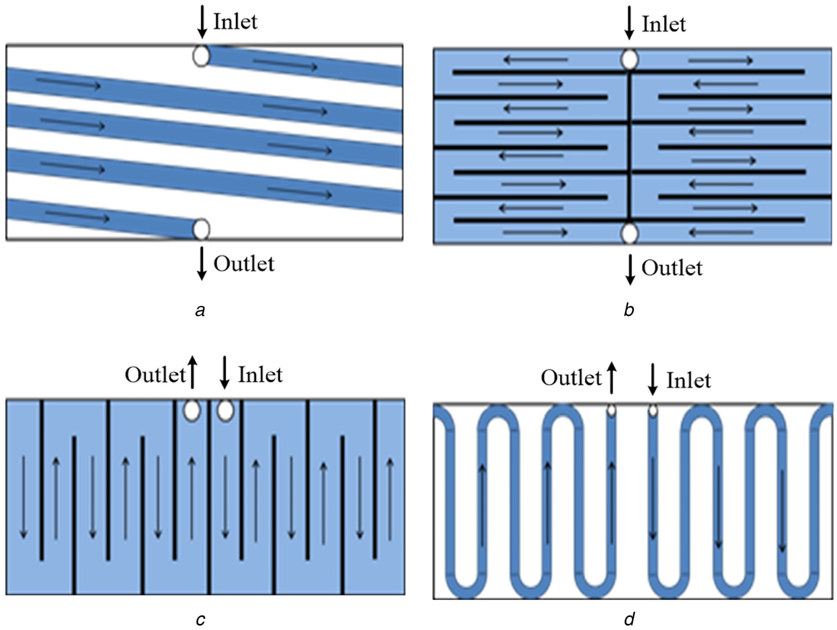

Fig. 10 *Various water jacket cooling configurations and paths*
(a) Helical channels, ***(b)*** Circumferential channels, ***(c)*** Meander axial channgels, ***(d)*** Axial Serpentine channels

cooling fluid [62, 63], or it can be the combination of the both [64, 65]. Fig. 9 illustrates the typical cooling technologies depending on cooling locations in electric machines.

Water jacket cooling is a commonly-used indirect cooling technique. It enables an effective heat transfer from the active part of stator to the coolant. The advantages of using water jacket include higher power-to-frame size ratio, lower noise level, higher efficiency, and completely enclosed environment. Also, the removed heat is not directly dissipated into the environment [66, 67]. Different configurations of water jacket channels and frame structures have been exploited including helical ducts, circumferential channels, meander shape of the ducts, and axial serpentine channels, as shown in Fig. 10. The configuration and the number of cooling paths determine the cooling efficiency as well as the pressure drop from the inlet to the outlet. Disadvantages of using water jacket for cooling include higher manufacturing cost, requirement for an auxiliary system to provide coolant, risk of corrosion inside the water circuit, risk of leaks, and more precautions with maintenance.

Direct stator core cooling applies where water jacket cooling is not sufficient and a significant temperature gradient might exist between the outer stator surface and the inner stator core. Direct cooling channels can be placed at the stator outer diameter adjacent to the housing to minimise the electro-magnetic impact on machine performance, or inside stator back iron to form direct contact between the coolant and the hot stator core. For the same pressure drop in the channels, the machine with direct stator core cooling channels has significantly lower average temperature in the stator back iron compared to the ones with indirect cooling technologies [68].

Placing the cooling channels in the stator slots with direct contact to the windings can also achieve good cooling effect [69,

Table 3 Rules of thumb for cooling type and heat transfer coefficients [4]

	Current density range, A/mm^2	Heat transfer coefficient, W/(m^2·K)	Cooling efficiency	System complexity	Energy cost
natural convection	1.5–5	5–10	low	simple	none
forced convection	5–10	10–300	medium	medium	low
liquid cool	10–30	50–20,000	high	complex	high

© The Institution of Engineering and Technology 2016

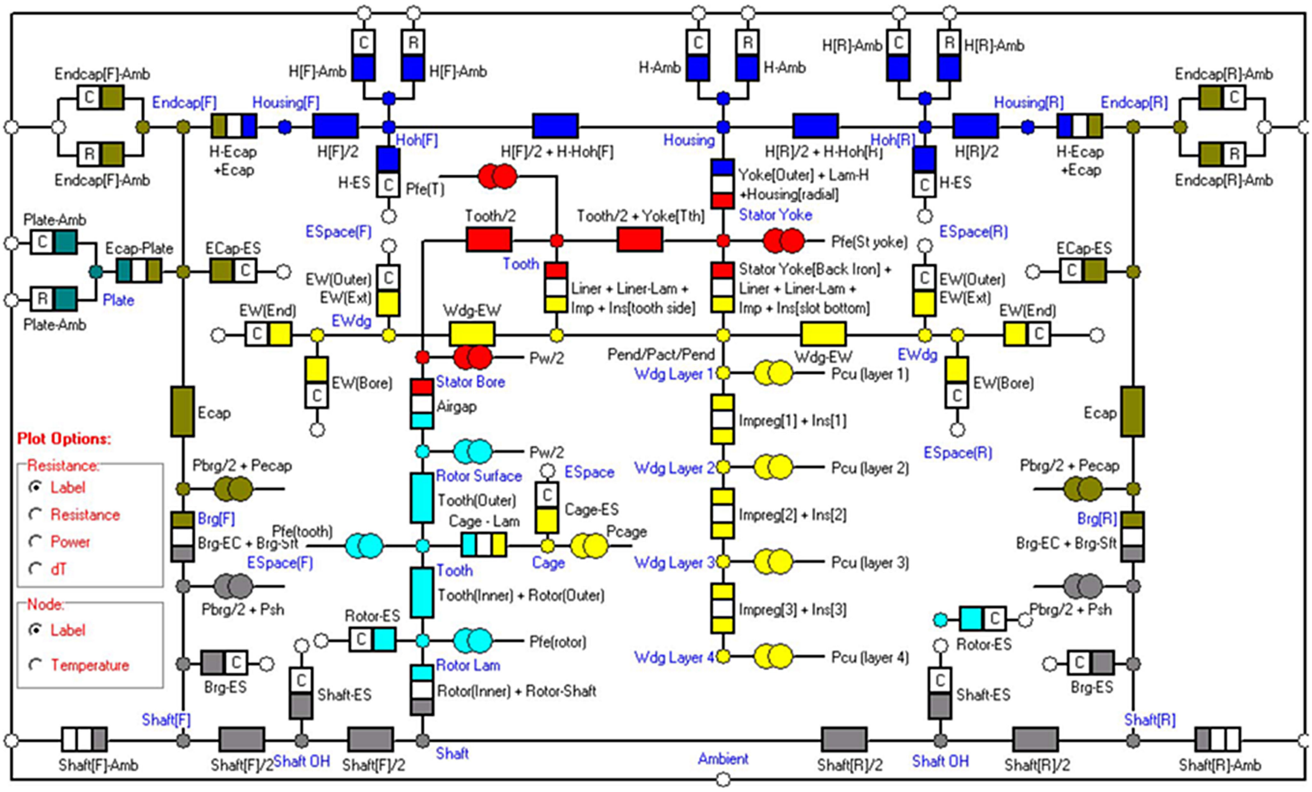

Fig. 11 *Example LPTN for an electric machine [18]*

70]. Furthermore, filling materials with high thermal conductivity, but low electromagnetic conductivity such as resin, epoxy, polymers, and thermoplastic can be applied to fill the winding gaps and allow better heat dissipation [71–73]. Direct winding heat exchanger utilising micro-feature enhanced meso-channels can be placed between two neighbouring winding coils in one slot to axially dissipate the heat generated from the windings, while the meso-channels allow for low pressure drop and high heat transfer coefficients [74].

Another critical location that sometimes requires additional cooling efforts in electric machines is the end winding. End winding cooling techniques include spray cooling, liquid jets and using thermally conductive material between the end windings and the frame. Due to the superior heat transfer characteristics of oil compared to water, oil may also be used as a cooling medium for spray cooling and liquid jets [75, 76].

Evaporative cooling is another effective cooling technique that uses two phase flow cooling systems to enhance heat dissipation of electric machine, which has been successfully applied in large electrical machines. This method has the perfect cooling capability and high reliability, but has the inconvenience of requiring very high quantity of coolant which makes it impractical for small size machines [77].

Other special cooling techniques have been developed. Piezoelectric fans are implemented to replace liquid cooling systems to improve fault-tolerance and reliability [78]. Temperature sensitive ferrofluids are used as cooling and dielectric medium for end winding to avoid extra complexity and costs in liquid cooling systems including deionised water, pumping system, filters, instrumentation and so on [79]. Totally immersed electrical machines are investigated such that the rotor and stator surfaces are directly flushed by hydraulic oil to increase the heat dissipation [80]. New machine geometry designs using stator flux-barriers for cooling are proposed to enhance the cooling area and, therefore, increase cooling efficiency [81].

6 Thermal analysis approaches

A key branch in the thermal management of electric machines is the ability to predict the temperature distribution during the design stage using thermal analysis approaches. Common methods for thermal analysis include lumped parameter thermal network (LPTN), FEA, and computational fluid dynamics (CFD).

6.1 LPTN analysis

The LPTN analysis offers a quick method of determining the temperature distribution within electric machines where the user can rapidly determine the changes resulting from different input parameters. Many publications have proven its application in various types of machine topologies including PM, induction, and SRMs. Commercially available software is capable of performing a thermal analysis using a LPTN approach.

The LPTN models usually consist of different components being lumped into simplified areas to represent more complex geometry [18, 82, 83]. The components can be lumped in different partial models such as radially in a 2D cross section of the machine, or a 3D layout taking into account the axial direction effects of heat distribution. Kim *et al.* [82] proposed a 2D LPTN which has three parallel paths for the heat to flow to the air. 2D LPTNs are used by El-Refaie *et al.* [84] and Lindström [83] where heat transfer is possible between the interior components, including interaction with the motor frame, and leading to the coolant channel. A similar network is given by Mellor *et al.* [85], but without forced cooling the heat leads from the frame to the ambient temperature. Alternatively, Securing Integrated Natural Nategh *et al.* [86] and Sali *et al.* [87] used 3D networks which allow heat transfer axially through the motor components instead of just through lumped cross sections. The 3D networks contain many additional nodes to encompass the different axial positions of components, as well as the front and back ends of the motor. One 3D LPTN of an electric motor from Boglietti *et al.* [18] is displayed in Fig. 11. The nodes located within each machine component represent the temperature of a lumped area. These temperature nodes are then connected with thermal resistances due to conduction, convection, or radiation. Thermal capacitance values are used to connect temperature nodes and ambient heat in the cases of transient thermal storage simulations [83]. Heat generation losses are found through analytical calculations, electromagnetic FEA studies, or experimental testing, and are then input into these nodal locations [18].

© The Institution of Engineering and Technology 2016

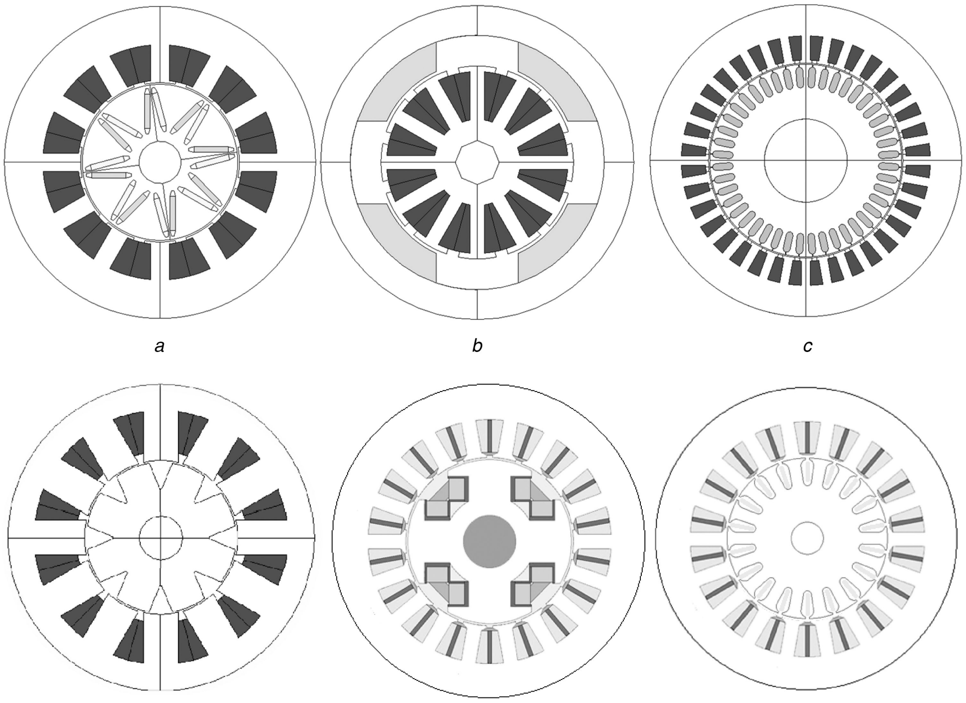

Fig. 12 *Examples of electric machine configurations*
(a) Brushless PM machine, *(b)* Brushed PM machine, *(c)* IM, *(d)* SRM, *(e)* Salient-pole SM, *(f)* Non-salient-pole SM

A LPTN is similar to that of an electrical circuit network, where voltage represents temperature, current represents heat flow, and electrical resistance and capacitance represent thermal resistance and capacitance, respectively [18]. Heat transfer coefficients, i.e. *h*-values, can be used to calculate the thermal resistances due to convection. Empirical formulas to calculate heat transfer coefficients have been developed for different areas of the motor such as across the air gap and heat transfer through the internal end space air [83, 88]. The *h*-values change based on the pattern, shape, rotational speed, and orientation of the applied cooling method and the surface area, which is in contact with.

The LPTN model can then predict the steady-state or transient heat flow within the electric machine, and the temperatures of each component. The more detailed the network is, the more accurately it can determine the temperatures of different areas within the machine. The temperatures predicted by the lumped parameter networks have been found to closely represent the same distribution as is found in FEA and CFD simulations as long as the machine is not overly complex. The results of changes in user inputs in the network are quickly found since the calculations are analytical and usually much less complex than that of FEA and CFD.

A downside to the LPTN method of thermal analysis is that it involves substantial effort to create an accurate model [18]. The LPTN provides a tool that can calculate the heat transfer and temperature distribution much quicker than CFD or FEA methods, but it can be very time consuming to create the thermal network [82–84]. Further efforts are required through validation and correction from either simulation or experimental measurement, and it is challenging to modify the LPTN to be applicable to various types of machines. In addition, the heat transfer between nodes is calculated based on the thermal properties of the materials and fluids, and with the temperature affecting the material properties, calibration is required to modify the thermal network to apply it to different operating conditions.

The geometry dimensions such as the number of poles, stator teeth, rotor teeth, and magnets, if applicable, will all affect the thermal circuit and resistances between connected nodes in the LPTN. The LPTN models for different machines vary depending on different stator and rotor configurations, which have key telltale difference and lead to different network path when building LPTN models.

6.1.1 Synchronous machine: This type of machine features a distributed armature winding that is located on the stator and distributed or concentrated field windings on the rotor. A DC current is driven in the field coils to generate DC magnetic field in the rotor. The presence of slotting, saliency, and the armature reaction (with current harmonics) add higher order flux harmonics that can result in high iron loss densities in proximity of the air gap [55]. The stator current produces copper losses that are similar to other AC machines. A DC/DC converter typically generates the rotor DC current using rotor inductance to smooth the current [89]. The resulting harmonics produce copper losses at the resulting frequencies. Some synchronous motors and grid-connected synchronous generators feature a third 'damper' winding that adds line-starting capabilities and prevents oscillations in the case of varying loads. During transients, this winding behaves similar to an IM rotor winding and results in similar loss mechanisms. In steady-state operation, current harmonics, e.g. due to an inverter, can cause significant copper losses in the damper winding [55]. The thermal analysis of SM using LPTN is an ongoing research topic with recent results in [90–92].

6.1.2 PM synchronous machine: In comparison to other types of machines, the PM machine consists of a rotor which contains embedded or surface mounted PMs. Magnetic losses are generated in the magnets which are applied to the LPTN. A LPTN which represents a PM machine will incorporate the quantity and dimensions of the magnets as well as its position within the rotor. The addition of the bonding or insulating material surrounding the magnets also changes the thermal resistance between magnets and the rotor due to conduction. Two examples of PM machines can be viewed in Figs. 12*a* and *b*. It should be noted that the brushes and commutators are placed at the end of the machine and thus not shown in Fig. 12*b* for the brushed PM DC machine. Many publications have demonstrated performing a thermal analysis of a PM machine using a LPTN [83, 93].

6.1.3 Induction machine: An IM incorporates a rotor core which either has squirrel-cage rotor bars or slots that contain coil windings, similar to those in the stator core. In the case of a squirrel-cage type rotor, the aluminium or copper bars are connected by end rings which short circuit the connections and generate copper losses as current is induced by the rotating stator

© The Institution of Engineering and Technology 2016

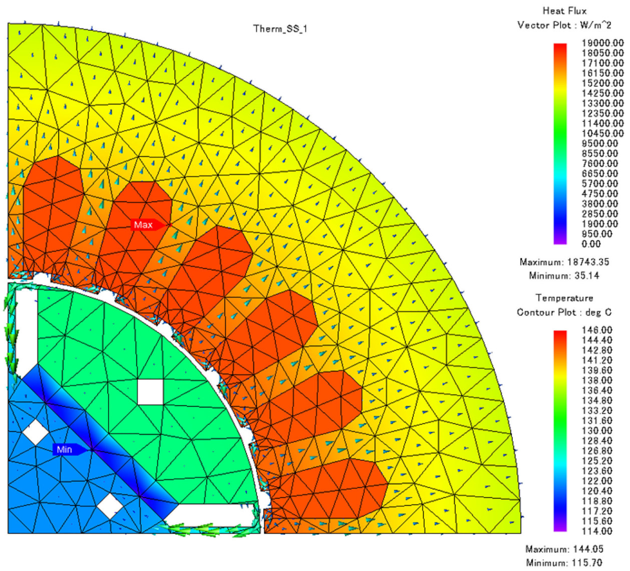

Fig. 13 *Example of a partial model FEA thermal analysis*

magnetic field. Meanwhile, eddy current and hysteresis losses are induced in the electrical steel laminations that are axially aligned through the rotor bars. Similarly with the wound-rotor, the coils in the rotor core generate secondary copper losses as current is induced. A LPTN designed for an IM will incorporate the addition of either the copper/aluminium bar or the coil material. Insulation around the coils and sleeves inserted in the rotor slots would also be incorporated and changes would be made to the thermal resistances due to conduction through the different material components. An example of an IM machine can be viewed in Fig. 12*c*. Many publications have demonstrated performing a thermal analysis of an IM using a LPTN [18, 88, 94].

6.1.4 Switched reluctance machine: Unlike the previous machine types, the rotor core of an SRM only consists of electrical steel material and does not contain any magnet or coil winding components. This allows for a more simplified LPTN as the radial thermal resistance due to conduction only passes through the rotor core material of certain dimensions. An example of an SRM machine can be viewed in Fig. 12*d*. Many publications have demonstrated performing a thermal analysis of an SRM using a LPTN [95, 96].

6.2 Numerical modelling methods

Numerical modelling methods exist which are also proven tools for predicting the temperature within electric machines when compared with experimental results. The two most common examples of numerical modelling methods are FEA and CFD. While these methods can be more accurate in predicting temperatures within electric machines with a low comparative error, they generally are more time consuming due to higher complexity and more detailed input components. Each thermal analysis type has its associated advantages and weaknesses.

6.2.1 FE analysis: FEA involves dividing the components within a model into many tiny meshed nodes and elements, to analyse the changes across those dimensions. Many examples of commercially available software are capable of performing 2D or 3D thermal FEA in both steady-state and transient simulations. Results found through thermal FEA are similar to that of LPTN models since common inputs are applied; however, the processing time is a downside of FEA. FEA thermal analysis has an advantage when the geometry becomes too complex to model using a LPTN [18].

2D simulations can be used to represent the temperatures within a machine when there is assumed to be little temperature difference across the axial components. FEA models are usually simplified to be partial fractional models, representative of the full geometry by applying periodic patterns, in order to speed up processing time. Heyns and Wang [58] apply an FEA partial model which observes 1/6 of the motor geometry. Zhang *et al.* [97] use a 3D geometry FEA electromagnetic and thermal linked model focusing specifically on the stator core to determine the temperature distribution. Marignetti *et al.* [98] use a 3D full model FEA coupled electromagnetic and thermal model to find the heat distribution through interior components including the windings, shaft, magnets, core and so on. Wu *et al.* [99] design a 1/8 partial model electromagnetic and thermal coupled FEA simulation for a switched reluctance motor, modelling the stator, windings, rotor, shaft, and magnets. Heat transfer coefficient values and heat resistances are required as inputs to calculate the convective heat transfer between surfaces and air or fluids. Losses and heat transfer boundary values are also inputs and are determined through analytical calculations, numerical simulations, or experimental testing [58]. Material properties of components and the geometrical dimensions determine the thermal resistance due to conduction within the machine. The more detailed the mesh that is applied to the model, the more accurate the temperature prediction will be, however the computational time will also increase with complexity. FEA thermal analysis can also be used to validate a LPTN model under development [58, 86]. An example of a partial model FEA thermal analysis for comparison with a LPTN model is displayed in Fig. 13.

6.2.2 CFD analysis: CFD is usually the most accurate temperature prediction method when compared with the LPTN and FEA methods. It can be used to determine heat transfer boundaries for inputs into LPTN and FEA methods, and has the ability to perform simulations to predict the fluid flow characteristics and optimise cooling methodologies (e.g. water jacket, air cooled etc.) [100].

Conventional CFD simulations only solve for the fluid flow and do not cover the solid domains. The losses values evaluated from electromagnetic calculations are incorporated into the CFD simulations as surface heat flux or constant surface temperatures boundary conditions. Several CFD thermal analyses with different levels of complexity were implemented to simulate the air flow around different components of the machine such as in the stator–rotor air gap [101, 102], end windings [103], or in cooling passages [104, 105]. Huang *et al.* [106] used steady-state CFD simulations characterise the heat transfer performance of three different shaped cooling channels for forced cooling in traction motors of hybrid electric vehicles and zero emission vehicles. The cooling channels were embedded in the stator core with oil as cooling fluid. The authors reported that the dimensional parameters developed can easily be applied to 2D or 3D FEA for thermal analysis or lumped parameter model analysis for the complete motor.

The simulation results can be improved by applying conjugate heat transfer method [105, 107], where the solid domains have to be modelled in addition to the fluid domains and the heat losses can be defined in the solid domains as volumetric sources obtained by electromagnetic simulations. Due to the advancement of the computational power in the recent years, using CFD conjugate thermal analysis for electric machines became a focus of several researchers [107, 108]. Previous research using conjugate CFD thermal analysis focused on air cooled systems [109–111], water or oil cooled systems [80, 112, 113] and hybrid systems [114]. In the recent study performed by Schrittwieser *et al.* [111], the authors compared between the simulation results based on a conjugate heat transfer model and those obtained by conventional heat transfer model (no conduction). The results showed that the temperature deviations between the two models are relatively small and that the conventional heat transfer model are generally applicable for calculating stator temperatures with the benefit of shorter calculation times.

CFD thermal analysis has the advantage in scenarios including when focusing on simultaneous air flows and mass transfer with a mix of laminar and turbulent states within a machine, and when designing channels and patterns for coolant flow [100]. Similar to how materials are input into geometry components in FEA, fluid properties and specifications are input in CFD, including volume flow rate, inlet temperatures, and pressure [18, 100]. Temperatures

© The Institution of Engineering and Technology 2016

of fluids can be resultant of change over time as opposed to being approximated during calculations for the initial conditions. However, a drawback to CFD thermal analysis is that simulation takes much longer to process depending on complexity of the geometry, degree of meshing, and the computational processing power available. This limits the user as they are not able to quickly observe the result of changes to input parameters in the design on the thermal distribution within the machine.

6.3 Experimental validation

Both lumped parameter thermal network analysis and numerical modelling methods provide profound insights and guidance in temperature prediction and thermal management of electric machines. However, certain degrees of error or inaccuracy always exist due to model limitation, parameter deviation, various assumptions, simplified boundary conditions and so on. Thus, it is often necessary to calibrate and verify the thermal analysis through experimental tests. In principle, two types of experiments are conducted. (i) Experiments that are designed to determine machine thermal parameters including thermal capacitance, thermal resistance, thermal conductivity, convection heat transfer coefficients, radiation heat transfer coefficients and so on. These can either be performed on complete machines to draw conclusions on similar machines and structures [115, 116], or on part of machines such as segmented stator structures [117] and end windings [118]. (ii) Experiments that are conducted to verify the analysis or simulation results, typically in the form of prototype machines.

In terms of temperature monitoring, direct thermal sensor measurements are widely applied on industrial applications and laboratory instrumentations at machine locations such as on the windings, end caps, housing, cooling jacket and so on [119, 120]. Typically used thermal sensors include thermocouples, thermistors, resistance thermometers and so on. Thermocouples are based on the principle that the junction of two dissimilar metals generates a voltage which increases with temperature. They have the advantages of high measurement range, fast response time, and simple configuration. However, they only have medium accuracy and sensitivity, and are prone to electromagnetic interference due to low signal strength. Thermistors are made of metal oxides whose resistances increase or decrease with increasing temperature, hence also called positive temperature coefficient or negative temperature coefficient sensors, respectively. Compared to thermocouples, thermistors provide more accurate, sensitive, robust signal output, and they have the advantages of simple construction, small size, low thermal mass, low cost, and being ineffective to electromagnetic noise. However, due to their narrow linear range, thermistors have limited useful temperature span [121]. Resistance thermometers, or resistance temperature detectors (RTDs), are similar to thermistors where they utilise resistances to measure temperature. The resistances of RTDs increase with temperature hence they are PTC sensors. RTDs are the most accurate, sensitive, and stable temperature sensors for industrial applications, although they are higher priced and require external power sources. In some cases, where direct sensor is difficult to access such as rotor and magnets, indirect temperature measurement is implemented by using infrared thermography, wireless communication, or slip-ring signal transmission [122–124]. Temperature estimation techniques based on flux observer, signal injection, lumped-parameter thermal networks have also been developed to ensure design redundancy in case of sensor failures [125–127].

7 Conclusion

Thermal management in electric machines plays a critical role in determining the machine performance and reliability. This paper comprehensively examines different aspects related to electric machine thermal management. Fundamental material thermal properties and loss generations have been discussed, diverse approaches for thermal analysis and cooling techniques have been presented, and various design considerations for thermal management have been provided. It is the purpose of this paper to serve as a reference guideline for machine designers who are interested in thermal management and thermal researchers who are interested in machine technologies.

8 Acknowledgments

This research was undertaken, in part, thanks to funding from the Canada Excellence Research Chairs program.

9 References

[1] Boldea, I., Tutelea, L.N.: '*Electric machines: steady state, transients, and design with MATLAB*' (CRC Press, Boca Raton, FL, 2009)

[2] Chapman, S.J.: '*Electric machinery fundamentals*' (McGraw-Hill, New York, NY, 2005, 4th edn.)

[3] Bilgin, B., Sathyan, A.: '*Fundamentals of electric machines', in Advanced electric drive vehicles*' in Emadi, A. (Ed.), (CRC Press, Boca Raton, FL, 2014), pp. 107–186

[4] Staton, D.: 'Thermal Analysis of Traction Motors'. Transportation Electrification Conf. and Expo (ITEC), Dearborn, MI, 2014

[5] Yang, Y., Arshad-Ali, K., Roeleveld, J., *et al.*: 'State-of-the-art electrified powertrains: hybrid, plug-in hybrid, and electric vehicles', *Int. J. Powertrains*, 2016, **5**, (1), pp. 1–28

[6] Hou, R., Yang, Y., Emadi, A.: 'Hybrid electric locomotive powertrains'. IEEE Transportation Electrification Asia-Pacific (ITEC Asia-Pacific), Beijing, 2014

[7] Yang, Y., Emadi, A.: 'Integrated electro-mechanical transmission systems in hybrid electric vehicles'. 2011 IEEE Vehicle Power and Propulsion Conf., Chicago, IL, September 2011

[8] Yang, Y., Schofield, N., Emadi, A.: 'Integrated electro-mechanical double-rotor compound hybrid transmissions for hybrid electric vehicles', *IEEE Trans. Veh. Technol.*, 2016, **65**, (6), pp. 4687–4699

[9] Emadi, A., Ehsani, M., Miller, J.M.: '*Vehicular electric power systems: land, sea, air, and space vehicles*' (Marcel Dekker Inc., New York, NY, 2004)

[10] Bilgin, B., Magne, P., Malysz, P., *et al.*: 'Making the case for electrified transportation', *IEEE Trans. Transp. Electrification*, 2015, **1**, (1), pp. 4–17

[11] Rogers, S.: '*EV everywhere grand challenge, electric drive status and challenges*' (U. S. Department of Energy, Energy Efficiency & Renewable Energy, 2012)

[12] Zhu, Z.Q., Howe, D.: 'Electrical machines and drives for electric, hybrid, and fuel cell vehicles', *Proc. IEEE*, 2007, **95**, (4), pp. 746–765

[13] Bilgin, B., Emadi, A.: 'Electric motors in electrified transportation: a step toward achieving a sustainable and highly efficient transportation system', *IEEE Power Electron. Mag.*, 2014, **1**, (2), pp. 10–17

[14] Bennion, K.: 'Electric Motor Thermal Management'. *National Renewable Energy Laboratory*, NREL Report No. PR-5400-50510, 2011

[15] Liao, C.M., Chen, C.L., Katcher, T.: 'Thermal analysis for design of high performance motors'. Int. Conf. on Thermal and Thermomechanical Phenomena in Electronic Systems, Seattle, WA, 1998

[16] Howey, D.A., Childs, P.R.N., Holmes, A.S.: 'Air-gap convection in rotating electrical machines', *IEEE Trans. Ind. Electron.*, 2012, **59**, (3), pp. 1367–1375

[17] Bennion, K., Cousineau, J.: 'Sensitivity study of traction drive motor cooling'. IEEE Transportation Electrification Conf. and Expo (ITEC), Dearborn, MI, 2012

[18] Boglietti, A., Cavagnino, A., Staton, D.A., *et al.*: 'Evolution and modern approaches for thermal analysis of electrical machines', *IEEE Trans. Ind. Electron.*, 2009, **56**, (3), pp. 871–882

[19] Moreno, G., Narumanchi, S., Bennion, K., *et al.*: 'Gaining traction: thermal management and reliability of automotive electric traction-drive systems', *IEEE Electrification Mag.*, 2014, **2**, (2), pp. 42–49

[20] Yang, R., Yang, Y., Bilgin, B., *et al.*: 'Analysis of interior permanent magnet machines with grain boundary diffusion processed magnet'. IET Int. Conf. on Power Electronics, Machines, and Drives (PEMD 2016), Glasgow, Scotland, 2016

[21] Toliyat, H.A., Kliman, G.B.: '*Handbook of electric motors*' (CRC Press, Boca Raton, FL, 2004)

[22] Bennion, K., Cousineau, J., Moreno, G.: 'Electric motor thermal management for electric traction drives'. SAE Thermal Management Systems Symp., Denver, CO, 2014

[23] Krishnamurthy, M., Edrington, C.S., Emadi, A., *et al.*: 'Making the case for applications of switched reluctance motor technology in automotive products', *IEEE Trans. Power Electron.*, 2006, **21**, (3), pp. 659–675

[24] Senda, K., Namikawa, M., Hayakawa, Y.: 'Electrical steels for advanced automobiles – core materials for motors, generators and high-frequency reactors'. *JFE Steel Tech. Rep.*, Tokyo, Japan, 2004

[25] Gerada, D., Mebarki, A., Brown, N.L., *et al.*: 'High-speed electrical machines: technologies, trends, and developments', *IEEE Trans. Ind. Electron.*, 2014, **61**, (6), pp. 2946–2959

[26] Nategh, S., Krings, A., Huang, Z., *et al.*: 'Evaluation of stator and rotor lamination materials for thermal management of a PMaSRM'. Int. Conf. on Electrical Machines (ICEM), Marseille, 2012

[27] Narumanchi, S.: 'Thermal management of power electronics and electric motors for electric-drive vehicles'. IEEE Energy Conversion Congress and Exposition (ECCE), Pittsburgh, PA, 2014

[28] Emadi, A.: '*Energy-efficient motors*' (CRC Press, Boca Raton, FL, 2004)

[29] Stone, G.C., Culbert, I., Boulter, W.A., *et al.*: '*Rotating machine insulation systems*' '*Electrical Insulation for Rotating Machines*' (IEEE Press, Hoboken, New Jersey, USA, 2014)

[30] 'National Electrical Manufacturers Association Standard'. ANSI/NEMA MW 1000-2015, 2015

© The Institution of Engineering and Technology 2016

[31] Marquez, E., Nelson, D.: 'Development of current squared – time curves for simplified wire size selection for electric traction systems in automotive applications'. IEEE Transportation Electrification Conf. and Expo, Dearborn, MI, June 2015
[32] 'Magnet Wire/Winding Wire Product Application and Packaging Data'. Superior Essex, 1999. Available at: http://www.superioressex.com/
[33] Beeckman, R.: 'NEMA magnet wire thermal class ratings'. Essex Group, Inc. Available at: http://www.superioressex.com/. [Accessed August 2015]
[34] 'Magnet wire insulation guide'. MWS Wire Industries. Available at: http://mwswire.com/, [Accessed 2016]
[35] Mechler, G.C.: 'Manufacturing and cost analysis for aluminum and copper die cast induction motors for GM's powertrain and R&D divisions'. *M.S. thesis, Department of Materials Science and Engineering*, Massachusetts Institute of Technology, Cambridge, MA, 2010
[36] '*NEOREC series neodymium iron boron magnet datasheet*'. TDK Corporation, May 2011. Available at: http://tdk.co.jp/
[37] Constantinides, S.: 'The demand for rare earth materials in permanent magnets'. Arnold Magnetic Technologies. Available at: http://arnoldmagnetics.com/, [Accessed 15 July 2015]
[38] Trout, S.R.: 'Material selection of permanent magnets, considering the thermal properties correctly'. Proc. the Electric Manufacturing and Coil Winding Conf., Cincinnati, OH, October 2001
[39] Tong, W.: '*Mechanical design of electric motors*' (CRC Press, Boca Raton, FL, 2014)
[40] Takahashi, N., Morishita, M., Miyagi, D.*, et al.*: 'Examination of magnetic properties of magnetic materials at high temperature using a ring specimen', *IEEE Trans. Magn.*, 2010, **46**, (2), pp. 548–551
[41] 'Selection of Electrical Steels for Magnetic Cores'. AK Steel. Available at: http://aksteel.com/, [Accessed 16 July 2015]
[42] 'Standard Classification of Insulating Coatings for Electrical Steels by Composition, Relative Insulating Ability and Application'. American Society of Testing and Materials, ASTM A 976-13, 2015
[43] 'DuPONT NOMEX Paper Type 410', DuPONT. Available at: http://www.dupont.com, [Accessed August 2015]
[44] Chang, C.C., Cheng, C.H., Ke, M.T.*, et al.*: 'Experimental and numerical investigations of air cooling for a large-scale motor', *Int. J. Rotating Mach.*, 2009, **2009**, pp. 1–7
[45] De Almeida, A.T., Ferreira, F.J.T.E.T.E., Fong, J.A.C.: 'Standards for efficiency of electric motors', *IEEE Ind. Appl. Mag.*, 2011, **17**, (1), pp. 12–19
[46] Nalakath, S., Preindl, M., Bilgin, B.*, et al.*: 'Modeling and analysis of AC resistance of a permanent magnet machine for online estimation purposes'. IEEE Energy Conversion Congress and Exposition, Montreal, QC, 2015
[47] Sudhoff, S.: '*AC conductor losses in power magnetic devices: a multi-objective design approach*' (Wiley-IEEE Press, 2014)
[48] Demetriades, G.D., De La Parra, H.Z., Andersson, E.*, et al.*: 'A real-time thermal model of a permanent-magnet synchronous motor', *IEEE Trans. Power Elctron.*, 2010, **25**, (2), pp. 463–474
[49] Zhang, Y., Cheng, M.C., Pillay, P.: 'Magnetic characteristics and excess eddy current losses'. Industry Applications Society Annual Meeting, Houston, TX, 2009
[50] Nalakath, S., Preindl, M., Yang, Y.*, et al.*: 'Modeling and analysis of core losses of an IPM magnet machine for online estimation purposes'. Annual Conf. of IEEE Industrial Electronics Society, Yokohama, Japan, 2015
[51] Mthombeni, T.L., Pillay, P.: 'Physical basis for the variation of lamination core loss coefficients as a function of frequency and flux density'. Annual Conf. on IEEE Industrial Electronics, Paris, November 2006
[52] Han, S., Jahns, T.M., Zhu, Z.Q.: 'Analysis of rotor core eddy-current losses in interior permanent magnet synchronous machines'. Industry Applications Society Annual Meeting, Edmonton, Alta, October 2008
[53] Ma, L., Sanada, M., Morimoto, S.*, et al.*: 'Prediction of iron loss in rotating machines with rotational loss included', *IEEE Trans. Magn.*, 2003, **39**, (4), pp. 2036–2041
[54] Ridge, A., McMahon, R., Kelly, H.P.: 'Detailed thermal modelling of a tubular linear machine for marine renewable generation'. IEEE Int. Conf. on Industrial Technology, Cape Town, 2013
[55] Rasilo, P., Belahcen, A., Arkkio, A.: 'Importance of iron-loss modeling in modelling in simulation of wound-field synchronous machines', *IEEE Trans. Magn.*, 2012, **48**, (9), pp. 2495–2504
[56] Deeb, R., Janda, M., Makki, Z.: 'Prediction of eddy current losses of surface mounted permanent magnet servo motor'. Int. Conf. on Electrical Machines, Marseille, September 2012
[57] Zhu, Z.Q., Ng, K., Schofield, N.*, et al.*: 'Improved analytical modelling of rotor eddy current loss in brushless machines equipped with surface-mounted permanent magnets', *IEE Proc. Electr. Power Appl.*, 2004, **151**, (6), pp. 641–650
[58] Heyns, G.C., Wang, R.-J.: 'Thermal analysis of a water-cooled interior permanent magnet traction machine'. IEEE Int. Conf. on Industrial Technology (ICIT), Cape Town, February 2013, pp. 416–421
[59] Miller, T.J.E.: '*SPEED's electric machines*' (CD-Adapco, 2002)
[60] Dessouky, Y.G., Williams, B.W., Fletcher, J.E.: 'Cooling enhancement of electric motors', *IEE Proc. Electr. Power Appl.*, 1998, **145**, (1), pp. 57–60
[61] Lee, Y., Hahn, S.Y., Kauh, S.K.: 'Thermal analysis of induction motor with forced cooling channels', *IEEE Trans. Magn.*, 2000, **36**, (4), pp. 1394–1397, Part 1
[62] Farsane, K., Desevaux, P., Panday, P.K.: 'Experimental study of the cooling of a closed type electric motor', *Appl. Therm. Eng.*, 2000, **20**, (14), pp. 1321–1334
[63] Li, H.: 'Cooling of a permanent magnet electric motor with a centrifugal impeller', *Int. J. Heat Mass Transf.*, 2010, **53**, (4), pp. 797–810
[64] Nakahama, T., Suzuki, K., Hashidume, S.*, et al.*: 'Cooling airflow in unidirectional ventilated open-type motor for electric vehicles', *IEEE Trans. Energy Convers.*, 2006, **21**, (3), pp. 645–651
[65] Mizuno, S., Noda, S., Matsushita, M.*, et al.*: 'Development of a totally enclosed fan-cooled traction motor', *IEEE Trans. Ind. Appl.*, 2013, **49**, (4), pp. 1508–1514
[66] Karim, Z.A.A., Yusoff, A.H.M.: 'Cooling system for electric motor of an electric vehicle propulsion', *Adv. Mater. Res.*, 2014, **903**, pp. 209–214
[67] Borges, S.S., Cezario, C.A., Kunz, T.T.: 'Design of water cooled electric motors using CFD and thermography techniques'. Int. Conf. on Electrical Machines, Vilamoura, Portugal, 2008
[68] Huang, Z., Nategh, S., Lassila, V.*, et al.*: 'Direct oil cooling of traction motors in hybrid drives'. IEEE Int. Electric Vehicle Conf. (IEVC), Greenville, SC, 2012
[69] Vlach, R., Grepl, R., Krejci, P.: 'Control of stator winding slot cooling by water using prediction of heating'. IEEE Int. Conf. Mechatronics (ICM), Kumamoto, 2007
[70] Galea, M., Gerada, C., Raminosoa, T.*, et al.*: 'A thermal improvement technique for the phase windings of electrical machines', *IEEE Trans. Ind. Appl.*, 2012, **48**, (1), pp. 79–87
[71] Yang, Y.: 'Double-rotor switched reluctance machine for integrated electro-mechanical transmission in hybrid electric vehicles'. *PhD dissertation*, McMaster University, Hamilton, ON, Canada, February 2014
[72] Yang, Y., Schofield, N., Emadi, A.: 'Double-rotor switched reluctance machine (DRSRM)', *IEEE Trans. Energy Convers.*, 2015, **30**, (2), pp. 671–680
[73] Rhebergen, C., Bilgin, B., Emadi, A.*, et al.*: 'Enhancement of electric motor thermal management through axial cooling methods: a materials approach'. IEEE Energy Conversion Congress and Exposition (ECCE), Montreal, Canada, 2015
[74] Semidey, S.A., Mayor, J.R.: 'Experimentation of an electric machine technology demonstrator incorporating direct winding heat exchangers', *IEEE Trans. Ind. Electron.*, 2014, **61**, (10), pp. 5771–5778
[75] Boglietti, A., Cavagnino, A.: 'Analysis of the endwinding cooling effects in TEFC induction motors', *IEEE Trans. Ind. Appl.*, 2007, **43**, (5), pp. 1214–1222
[76] Staton, D.A., Popescu, M., Hawkins, D.*, et al.*: 'Influence of different end region cooling arrangements on end-winding heat transfer coefficients in electrical machines'. IEEE Energy Conversion Congress and Exposition, Atlanta, GA, 2010
[77] Guechi, M.R., Desevaux, P., Baucour, P.*, et al.*: 'On the improvement of the thermal behavior of electric motors'. IEEE Energy Conversion Congress and Exposition, Denver, CO, 2013
[78] Gilson, G.M., Pickering, S.J., Hann, D.B.*, et al.*: 'Piezoelectric fan cooling: a novel high reliability electric machine thermal management solution', *IEEE Trans. Ind. Electron.*, 2013, **60**, (11), pp. 4841–4851
[79] Karimi-Moghaddam, G., Gould, R.D., Bhattacharya, S.*, et al.*: 'Thermomagnetic liquid cooling: A novel electric machine thermal management solution'. IEEE Energy Conversion Congress and Exposition (ECCE), Pittsburgh, PA, 2014
[80] Ponomarev, P., Polikarpova, M., Pyrhönen, J.: 'Thermal modeling of directly-oil-cooled permanent magnet synchronous machine'. Int. Conf. on Electrical Machines (ICEM), Marseille, 2012
[81] Nollau, A., Gerling, D.: 'Novel cooling methods using flux-barriers'. Int. Conf. on Electrical Machines (ICEM), Berlin, 2014
[82] Kim, D.J., Jung, J.W., Kwon, S.O.*, et al.*: 'Thermal Analysis using Equivalent Thermal Network in IPMSM'. 2008 Int. Conf. on Electric Machines and Systems, Wuhan, China, 2008
[83] Lindström, J.: '*Development of an experimental permanent-magnet motor drive*' (Department of Electric Power Engineering, Göteborg, 1999)
[84] El-Refaie, A.M.H.N.C.a.J.T.M.: 'Thermal analysis of multibarrier interior PM synchronous machine using lumped parameter model', *IEEE Trans. Energy Convers.*, 2004, **19**, (2), pp. 303–309
[85] Mellor, P.H., Roberts, D., Turner, D.: 'Lumped parameter thermal model for electrical machines of TEFC design'. *IEEE Proc. B-Electr. Power Appl.*, 1991, **138**, (5), pp. 205–218
[86] Nategh, S., Wallmark, O., Leksell, M.*, et al.*: 'Thermal analysis of a PMaSRM using partial FEA and lumped parameter modeling', *IEEE Trans. Energy Convers.*, 2012, **27**, (2), pp. 477–488
[87] Sali, N.V.a.K.P.: 'Lumped parameter analysis of SMPM synchronous electric motor used for hybrid electric vehicle traction drive', *IOSR J. Mechan. Civil Eng.*, 2014, **2014**, pp. 42–47
[88] Staton, D., Boglietti, A., Cavagnino, A.: 'Solving the more difficult aspects of electric motor thermal analysis'. IEEE Int. Electric Machines and Drives Conf., 2003. IEMDC'03, Madison, 2003
[89] Illiano, E.: 'Design of a highly efficient brushless current excited synchronous motor for automotive purposes'. *PhD thesis*, ETH, Zurich, 2014
[90] Mejuto, C.: 'Improved lumped parameter thermal modelling of synchronous generators'. *PhD thesis, The University of Edinburgh*, 2010
[91] Nategh, S.: 'Thermal analysis and management of high-performance electrical machines'. *PhD thesis*, KTH, 2013
[92] Shafaie, R., Kalantar, M., Gholami, A.: 'Thermal analysis of 10-MW-class wind turbine HTS synchronous generator', *IEEE Trans. Appl. Supercond.*, 2014, **24**, (2), pp. 90–98
[93] Junak, J., Ombach, G., Staton, D.A.: 'Permanent magnet DC motor brush transient thermal analysis'. 2008 Int. Conf. on Electrical Machines, Vilamoura, 2008
[94] Cossar, C., McGilp, M., Omori, S.*, et al.*: 'Analytical thermal models for small induction motors'. 18th Int. Conf. on Electrical Machines, Vilamoura, 2008
[95] Tang, Y.: 'Characterization, numerical analysis, and design of switched reluctance motors', *IEEE Trans. Ind. Appl.*, 1997, **33**, (6), pp. 1544–1552
[96] Faiz, J., Ganji, B., Carstensen, C.E.*, et al.*: 'Temperature rise analysis of switched reluctance motors due to electromagnetic losses', *IEEE Trans. Magn.*, 2009, **45**, (7), pp. 2927–2934

© The Institution of Engineering and Technology 2016

[97] Zhang, Y., Ruan, J., Huang, T., *et al.*: 'Calculation of temperature rise in air-cooled induction motors through 3-D coupled electromagnetic fluid-dynamical and thermal finite-element analysis', *IEEE Trans. Magn.*, 2012, **48**, (2), pp. 1047–1050

[98] Marignetti, F., Colli, V.D., Coia, Y.: 'Design of axial flux PM synchronous machines through 3-D coupled electromagnetic thermal and fluid-dynamical finite-element analysis', *IEEE Trans. Ind. Electron.*, 2008, **55**, (10), pp. 3591–3601

[99] Wu, W., Dunlop, J.B., Collocott, S.J., *et al.*: 'Design optimization of switched reluctance motor by electromagnetic and thermal finite element analysis'. Digest of INTERMAG 2003. Int. Magnetics Conf., vol. **39**, no. 5, 2003, pp. 3334–3336

[100] Srinivas, K.N., Arumugam, R.: 'Analysis and characterization of switched reluctance motors: part ii - flow, thermal and vibration analyses', *IEEE Trans. Magn.*, 2005, **41**, (4), pp. 1321–1332

[101] Pickering, S.J., Lampard, D., Shanel, M.: 'Ventilation and heat transfer in a symmetrically ventilated salient pole synchronous machine'. Int. Conf. Power Electronics, Machines and Drives, June 2002

[102] Howey, D.A., Holmes, A.S., Pullen, K.R.: 'Measurement and CFD prediction of heat transfer in air-cooled disc-type electrical machines', *IEEE Trans. Ind. Appl.*, 2011, **47**, (4), pp. 1716–1723

[103] Connor, P.H., Pickering, S.J., Gerada, C., *et al.*: 'Computational fluid dynamics modelling of an entire synchronous generator for improved thermal management', *IET Electr. Power Appl.*, 2013, **7**, (3), pp. 231–236

[104] Wrobel, R., Vainel, G., Copeland, C., *et al.*: 'Investigation of mechanical loss components and heat transfer in an axial-flux pm machine', *IEEE Trans. Ind. Appl.*, 2015, **51**, (4), pp. 3000–3011

[105] Schrittwieser, M., Marn, A., Farnleitner, E., *et al.*: 'Numerical analysis of heat transfer and flow of stator duct models', *IEEE Trans. Ind. Appl.*, 2014, **50**, (1), pp. 226–233

[106] Huang, Z., Marquez, F., Alakula, M., *et al.*: 'Characterization and application of forced cooling channels for traction motors in HEVs'. 20th Int. Conf. on Electrical Machines (ICEM), 2012

[107] Shanel, M., Pickering, S.J., Lampard, D.: 'Conjugate heat transfer analysis of a salient pole rotor in an air cooled synchronous generator'. IEEE Int. Conf. of Machines and Drives, 2003

[108] Maynes, B.D.J., Kee, R.J., Tindall, C.E., *et al.*: 'Simulation of airflow and heat transfer in small alternators using CFD'. IEEE Proc. Electrical Power Applications, 2003

[109] Ujiie, R., Arlitt, R., Etoh, H.: 'Application of computational fluid dynamics (CFD) on ventilation-cooling optimization of electrical machines'. Review Energy Technologies Generation, Transmission and Distribution of Electric and Thermal Energy, 2006

[110] Nollau, A., Gerling, D.: 'A new cooling approach for traction motors in hybrid drives'. IEEE Int. Electric Machines and Drives Conf. (IEMDC), 2013

[111] Schrittwieser, M., Bíró, O., Farnleitner, E., *et al.*: 'Analysis of temperature distribution in the stator of large synchronous machines considering heat conduction and heat convection', *IEEE Trans. Magn.*, 2015, **51**, (3), pp. 49–53

[112] Jungreuthmayer, C., Bäuml, T., Winter, O., *et al.*: 'A detailed heat and fluid flow analysis of an internal permanent magnet synchronous machine by means of computational fluid dynamics', *IEEE Trans. Ind. Electron.*, 2012, **59**, (12), pp. 4568–4578

[113] Pechanek, R., Bouzek, L.: 'Analyzing of two types water cooling electric motors using computational fluid dynamics'. Int. Power Electronics and Motion Control Conf. (EPE/PEMC), 2012

[114] Polikarpova, M., Ponomarev, P., Lindh, P., *et al.*: 'Hybrid cooling method of axial-flux permanent-magnet machines for vehicle applications', *IEEE Trans. Ind. Electron*, 2015, **62**, (12), pp. 7382–7390

[115] Boglietti, A., Cavagnino, A., Staton, D.A.: 'Determination of critical parameters in electrical machine thermal models', *IEEE Trans. Ind. Appl.*, 2008, **44**, (4), pp. 1150–1159

[116] Yoheswaran, B., Pullen, K.R.: 'Flow and convective heat transfer in disk-type electric machines with coolant flow'. Int. Conf. on Electrical Machines (ICEM), 2014

[117] Wrobel, R., Mellor, P.H., Holliday, D.: 'Thermal modeling of a segmented stator winding design', *IEEE Trans. Ind. Appl.*, 2011, **47**, (5), pp. 2023–2030

[118] Boglietti, A., Cavagnino, A., Staton, D.A., *et al.*: 'End space heat transfer coefficient determination for different induction motor enclosure types', *IEEE Trans. Ind. Appl.*, 2009, **45**, (3), pp. 929–937

[119] Yang, Y., Schofield, N., Emadi, A.: 'Double-rotor switched reluctance machine design, simulations, and validations', *IET Electr. Syst. Transp.*, 2016, **6**, (2), pp. 171–175

[120] Cavagnino, A., Tenconi, A., Vaschetto, S.: 'Experimental characterization of a belt-driven multiphase induction machine for 48-V automotive applications: losses and temperatures assessments', *IEEE Trans. Ind. Appl.*, 2016, **52**, (2), pp. 1321–1330

[121] Michalski, L.: '*Temperature measurement*' (John Wiley & Sons, New York, 2001)

[122] Ganchev, M., Kubicek, B., Kappeler, H.: 'Rotor temperature monitoring system'. Int. Conf. on Electrical Machines (ICEM), 2010

[123] Mejuto, C., Mueller, M., Shanel, M., *et al.*: 'Improved synchronous machine thermalmodelling'. Int. Conf. on Electrical Machines (ICEM), 2008

[124] Stipetic, S., Kovacic, M., Hanic, Z., *et al.*: 'Measurement of excitation winding temperature on synchronous generator in rotation using infrared thermography', *IEEE Trans. Ind. Electron.*, 2012, **59**, (5), pp. 2288–2298

[125] Specht, A., Wallscheid, O., Böcker, J.: 'Determination of rotor temperature for an interior permanent magnet synchronous machine using a precise flux observer'. Int. Power Electronics Conf. (ECCE-Asia), Hiroshima, Japan, 2014

[126] Reigosa, D.D., Briz, F., Garcia, P., *et al.*: 'Magnet temperature estimation in surface PM machines using high-frequency signal injection', *IEEE Trans. Ind. Appl.*, 2010, **46**, (4), pp. 1468–1475

[127] Wallscheid, O., Böcker, J.: 'Global identification of a low-order lumped-parameter thermal network for permanent magnet synchronous motors', *IEEE Trans. Energy Convers.*, 2016, **36**, (1), pp. 354–365

© The Institution of Engineering and Technology 2016